Thermal degradation of n-hexadecane base oil and its impact on boundary friction and surface adsorption†

Sophie Campen[1], Chun Wai Jan Fong[2], Wei Song[1,3], Janet S. S. Wong[1]*

[1] Department of Mechanical Engineering, Imperial College London, London SW7 2AZ, UK.

[2] Department of Mechanical Engineering, City University of Hong Kong, 83 Tat Chee Avenue, Kowloon Tong, Hong Kong

[3] Fine Chemical Industry Research Institute, School of Chemistry, Sun Yat-sen University, Guangzhou, 510275, China

* Corresponding author j.wong@imperial.ac.uk

†All work was conducted at Imperial College London

Abstract

The chemical and physical properties of lubricants can alter during use. High temperatures may cause thermal autooxidation of the base oil, which could impact the performance of lubricant additives. Here, the effect of high temperature on the properties of n-hexadecane base oil is investigated. n-Hexadecane undergoes an irreversible transition from high to low boundary friction at 122-134°C when heated in air. FTIR, UV-vis and NMR spectroscopy indicate the presence of carbonyl- and hydroxyl-containing oxidation products (carboxylic acids, alcohols, esters, ketones and aldehydes). ATR-FTIR shows that iron carboxylates form exclusively inside and around the rubbed friction surface. QCM-D is used to investigate the adsorption of degradation products onto an iron(III) oxide surface and reveals that almost half the adsorbed mass is effectively irreversibly adsorbed.

Keywords

Degradation: Thermal, Lubrication: Boundary, Surface: Chemical analysis, Tribochemistry

1 Introduction

During automotive engine operation, high temperatures experienced in use may result in thermal degradation of engine oil. This thermal degradation alters the chemical and physical properties of the oil, which impacts its performance.[1] One of the main ways in which an engine oil may thermally degrade is by oxidation of the base oil. Hydrocarbon base oils contain various proportions of alkanes,

alkenes, cycloalkanes, aromatics and heteroatom-containing molecules.[2] Different base oils display different thermal stabilities owing to their different chemical compositions. For example, alkanes reportedly undergo rapid autooxidation, while aromatics reduce the rate of oxidation by acting as antioxidants.[3] Synthetic oils, such as polyalphaolefins (PAOs), tend to have higher thermal stability than mineral oils.[4,5]

It is well-documented that hydrocarbon autooxidation follows a radical pathway.[6–11] The first step, initiation, is the reaction of hydrocarbon with oxygen to form hydroperoxides. Subsequent reactions yield aldehydes, carboxylic acids, alcohols, ketones and esters. A recent study using advanced mass spectrometry has revealed that under certain conditions complex and highly oxidised molecules containing multiple peroxide groups can form.[12] Organometallic and high molecular weight polymeric species have also been observed, the latter likely form due to polymerisation reactions of α,β-unsaturated carbonyls.[13,14] These molecules may be responsible for the formation of insoluble precipitates in the liquid phase called ‘sludges’ and thick deposits on surfaces, often referred to as lacquers or varnishes.[3,15,16]

Metals can play a catalytic role in the autooxidation of hydrocarbons.[15,17] As engine parts are mostly made of steel, the role of iron is of particular interest. Iron is used as a homogeneous catalyst in Fenton’s reagent, a mixture of hydrogen peroxide with iron(II) salt, where it enables the disproportionation of hydrogen peroxide to yield hydroxyl and hydroperoxyl radicals, as well as water.[18] During the reaction, iron(II) is oxidised to iron(III) before being reduced back to iron(II). In heterogeneous Fenton reactions, the solid iron surface acts as a true heterogeneous catalyst while also leaching iron ions into the liquid which then participates in homogeneous Fenton reactions.[19] Recently it was shown that iron(II), iron(III) and iron(0) surfaces play different roles in the thermal autoxidation of n-hexadecane at 200 °C.[20] Iron(0) surfaces appeared particularly reactive, being involved in extensive n-hexadecane oxidation. Regardless of the initial surface chemistry, the final surface chemistry after thermal autooxidation was iron(III) oxide-hydroxide.

In addition to the catalytic role of the steel surface, the tribological contact can increase oxidation of oils relative to that obtained at elevated temperature alone. The induction time for the formation of hydroperoxides was found to be much shorter during tribo-oxidation, than by thermal autooxidation alone.[21] Nascent surfaces generated by wear of the uppermost surface of steel yields reactive iron centres. Attrition of the surface can generate ferrous particles as wear debris which may be dispersed within the liquid lubricant or deposited onto surfaces. This increases the available surface area to participate in heterogeneous catalysis of n-hexadecane oxidation. Additionally, iron centres which have reacted with carboxylic acids may form iron carboxylate salts and these, if dissolved in the oil, may perhaps participate in homogeneous catalysis of hexadecane oxidation.[22] The frictional contact may also aid the removal of adsorbed / deposited degradation products. This may help facilitate further reactions at the metal surface by limiting any inhibiting effect of the deposited film. Additionally, the tribological contact may increase the rate of oil oxidation if reactions can be partly

shear-stress activated.[23,24] Frictional heat and local temperature spikes generated within the rubbing contact can also promote oil oxidation.

Long chain alcohols, carboxylic acids and esters are known to reduce boundary friction when added to pure n-hexadecane in sufficiently high concentrations.[25–27] Thus, the products of base oil degradation may also reduce boundary friction. In an early study using the Bowden-Leben apparatus, white mineral oil gave stick-slip motion at temperatures of 15 and 100 °C, but continuous sliding at 200 °C.[28] Oil heated to 200°C in air and subsequently cooled to room temperature also exhibited continuous sliding, proving that the transition was irreversible and due to oil oxidation. Thick films of deposited oxidation products which coat surfaces, such as varnishes, may, however, result in increased friction. A non-negligible fraction, up to 20%, of old, degraded oil remains after an engine oil change, thus degradation products are likely to be present at some concentration in most engine oils.[29] Thermal autooxidation of the base oil has knock-on effects on the performance of lubricant additives existing in the formulated engine oil. Organic friction modifiers, which rely on adsorption to the surface to be effective, can be impacted by thermal autoxidation of the oil in numerous ways, including by competition for surface sites.

In this study we investigate the impact of high temperature on the properties of n-hexadecane base oil. n-hexadecane has previously been employed as a model component for both lubricant and fuel studies.[30–32] Firstly, the friction of n-hexadecane is monitored during a sliding friction test carried out at increasing temperature from 100 to 150 °C. Samples of thermally degraded n-hexadecane are prepared by heating n-hexadecane in air on a hotplate. These samples are analysed using UV-vis, FTIR and NMR spectroscopies and their viscosities measured. The friction and wear behaviour of thermally degraded n-hexadecane is compared with that of an n-hexadecane sample which is degraded in situ during a friction test carried out at an elevated temperature of 150°C. ATR-FTIR is used to analyse the surface of a steel disc after the test at elevated temperature to reveal the different chemistries existing both inside and outside the friction surface. The adsorption of n-hexadecane degradation products onto an Fe_2O_3 surface is investigated using quartz crystal microbalance with dissipation monitoring (QCM-D). The aim of this work is to relate the observed friction response of thermally degraded hexadecane to chemical changes occurring in the oil. Note that the thermally degraded n-hexadecane prepared here is used in a further study where its impact on the performance of organic friction modifier additive is investigated.

2 Experimental

2.1 Materials and preparation methods

n-Hexadecane (99%, Merck Millipore), used as a model base oil, was cleaned with alumina (Sigma-Aldrich, Brockmann Activity I, neutral) and silica (Sigma-Aldrich, for column chromatography) molecular sieves to remove any polar species, then stored over alumina in a dark cupboard at

ambient temperature (21°C). Immediately before use, hexadecane was filtered to remove alumina. Toluene (99.9 %, CHROMASOLV), 2-propanol (99.9%, CHROMASOLV), acetone (≥99.8%, CHROMASOLV), and n-heptane (≥99%, CHROMASOLV) solvents, used for cleaning, were acquired from Sigma-Aldrich.

Balls and discs of AISI 52100 bearing steel, used for friction tests, were acquired from PCS Instruments. Balls of 6 mm diameter had areal RMS roughness (S_q) of 22 ±3 nm and were through-hardened to 760 VPN. Discs had areal RMS roughness of 5 ±1 nm and were through-hardened to 800 HV. Average surface roughness values were obtained for clean unused specimens using an Olympus Lext 3D Laser Scanning Microscope. Before use, steel specimens were cleaned by rubbing with (i) toluene- and (ii) 2-propanol-wetted paper to remove any protective anti-corrosion film. Specimens were then placed in a screw-cap container filled with toluene and ultrasonicated for 30 min. After this time the specimens were rinsed with toluene and acetone and dried under a stream of nitrogen. Fe_2O_3-coated sensors of AT-cut quartz with 5 MHz fundamental frequency, used for QCM-D measurements, were acquired from Q-Sense. Before use, the sensors were ultrasonicated for 20 min in toluene, rinsed with toluene and isopropanol, dried in air, and cleaned in a low-pressure plasma cleaner under O_2 (Diener Electronic).

2.2 Friction testing

Friction tests were carried out using a High Frequency Reciprocating Rig (HFRR) from PCS Instruments, Acton, UK. During friction tests, a clamped steel ball was slid forwards and backwards in a reciprocating motion against the flat surface of a fixed steel disc. A stroke length of 1 mm and frequency of 50 Hz was used for all tests, giving an average sliding speed of 0.1 ms^{-1}. A load of 4 N was used, resulting in an initial mean Hertzian contact pressure of 0.69 GPa. HFRR friction experiments are carried out in the boundary lubrication regime, and given the reciprocating motion of ball, the sliding speed is not constant along the stroke length. Note, using the Hamrock-Dowson equation and assuming a pressure viscosity coefficient for hexadecane of 11.6 GPa^{-1}, the minimum film thickness at mid stroke is estimated to be 0.7 nm at a temperature of 100°C (dynamic viscosity = 0.898 mPa·s).[33–35] Given the composite surface roughness of 23 ±3 nm, a lambda ratio of 0.03 is obtained, well within the boundary lubrication regime (lambda ratio < 1).

A fixed lubricant volume of 2 mL was used for each test. A heating block, located directly beneath the disc sample holder, allowed heating during the test. Before sliding commenced, the lubricant sample and specimens were heated to the target temperature. Tests were made at (i) variable temperature, where heating and cooling took place during sliding, and (ii) constant temperature. Heating and cooling rates were 1°C min^{-1}. A temperature sensor inserted into the disc sample holder gave feedback and allowed temperature control during the test. During the test, the lubricant sample was open to the air. Any generated volatiles may thus be lost by evaporation. The electrical contact resistance (ECR) between the ball and disc gives an approximate measure of the boundary

lubricating film thickness as a percentage rather than a distance (e.g. in nm). An ECR measurement of 100% suggests that an insulating film exists between the ball and the disc and that the metal surfaces are not in direct contact, while an ECR measurement of 0% suggests that the ball and disc are in direct contact. For ECR measurements, a resistor value of 10 Ω was used for all tests.

Post-friction test, specimens were rinsed with n-heptane solvent to remove excess lubricant, then allowed to dry in air. A Zeiss optical microscope with camera attachment was used to obtain images of the friction surfaces on the ball and disc.

2.3 Controlled thermal degradation of n-hexadecane

n-Hexadecane was thermally degraded by heating in air on a hotplate with stirring. An IKA HS-7 C-MAG magnetic stirrer was used with ETS-D5 temperature probe. A sample of clean n-hexadecane (80 mL) was placed in a borosilicate glass beaker with 5 cm internal diameter giving an air-liquid interfacial area of 19.6 cm^2 at rest, prior to stirring. The initial liquid depth was 4.2 cm. A 15 mm length PTFE-coated stirrer bar with pivot ring was used to stir the liquid. Stirrer speed was increased to c. 600 rpm so that a stable vortex formed while maintaining smooth rotation of the stirrer bar and ensuring no liquid splashing. The temperature probe was inserted into the liquid and the temperature setpoint entered to control the hotplate. The liquid temperature was verified with a separate thermometer. Stirrer speed was adjusted as required during heating to ensure no splashing occurred because of the lower liquid viscosity at elevated temperature. Once the temperature had stabilized at the desired setpoint, the sample was typically degraded for 1 hour and aliquots (~ 3 mL) taken at approximately 10 min intervals using glass pipettes. Once thermal aging was complete, the heater was turned off, and the sample left stirring until it reached ambient temperature. The degraded sample and aliquots were stored in borosilicate jars sealed with polypropylene caps and kept in a dark cupboard. During aging, sources of light (which may promote degradation)[36,37] were not removed and typical laboratory lighting was used. A condenser was not attached, and heating was not carried out under reflux, this may have resulted in the loss of some light components (volatiles), if created during degradation.

2.4 UV-vis, FTIR and NMR spectroscopy

Ultraviolet-visible (UV-vis) and Fourier Transform Infrared (FTIR) spectra were obtained of both the original and degraded hexadecane samples. UV-vis spectra were obtained using a USB4000-UV−vis spectrometer with fibre optic light source (Ocean Optics). Samples were held in quartz cuvettes with 10 mm path length (Hellma Analytics). Transmission FTIR spectra were obtained using a Frontier spectrometer from Perkin-Elmer. Samples were prepared either by sandwiching directly between KBr optical windows to give a thin squeeze film or by injecting into a Specac Omni cell with PTFE spacer

and KBr windows to give a fixed 1 mm pathlength. Spectra were obtained for the range 4000 – 400 cm^{-1} at a resolution of 4 cm^{-1} and were averaged over 50 scans. A background spectrum was taken prior to sample measurements and acquired spectra were baseline-corrected in Spectrum software (Perkin-Elmer).

Attenuated total reflection (ATR)-FTIR spectra were obtained of a clean steel disc and the post-friction test surface. Before FTIR, the HFRR disc was rinsed with n-heptane to remove excess lubricant. The same Frontier spectrometer was used with a Multiscope FTIR microscope and a germanium crystal micro-ATR attachment (Perkin-Elmer). A background spectrum was acquired in air. Spectra were obtained for the range 4000 – 400 cm^{-1} at a resolution of 4 cm^{-1} and were averaged over 100 scans.

^1H NMR spectra were obtained of clean hexadecane and thermally degraded hexadecane. Samples were prepared in $CDCl_3$ (99.8 atom % D, Sigma-Aldrich) and spectra were acquired using a 400 MHz NMR spectrometer (Av 400) from Bruker. Offline analysis was carried out using MestReNova software.

2.5 Viscosity measurements

The viscosity and density of clean and thermally degraded n-hexadecane were measured using a Stabinger Viscometer (Anton Parr SVM 3000). Measurements were made at temperatures from 20-100°C at 10°C intervals. Before each sample was introduced, the viscometer was cleaned by injecting toluene and 2-propanol, then drying with pumped air.

2.6 QCM-D measurements

QCM-D (quartz crystal microbalance with dissipation monitoring) was used to investigate the adsorption of n-hexadecane thermal degradation products onto an Fe_2O_3 surface. A QSense E1 QCM-D with temperature-controlled flow cell (Biolin Scientific) was used with a Ismatec Reglo peristaltic pump (Cole-Parmer, UK). Liquids were pulled from a reservoir to the QCM, then passed through the pump before flowing out to a waste reservoir. The wetted materials in the flow path were of PTFE (tubing), PEEK (fittings), ETFE (ferrules), Kalrez (O-ring and gasket) and titanium (flow cell). The sensor's resonance frequencies (f_n) and dissipations (D_n) for overtones (n) 1, 3, 5, 7, 9, 11 and 13 were obtained in air. Clean n-hexadecane was flowed through the cell until stable baselines were achieved ($\Delta f_n/n$ < 0.5 Hz in 20 min), before flowing thermally degraded n-hexadecane (adsorption) and finally clean n-hexadecane (rinsing). Owing to the slightly different viscosity and density of the test liquids, the data was corrected for liquid loading effects before calculating adsorbed mass, as described previously.[38,39]

3 Results and discussion

3.1 Variable temperature friction experiment

The friction of clean n-hexadecane was investigated during a heating-cooling cycle, see Fig 1. Initially the temperature was held constant at 100 °C for a period of 30 min. The average friction coefficient is relatively high (0.23) and the ECR is 0%. (Note that a friction coefficient of c. 0.1 is typical for an effective boundary lubricating film). This suggests that a boundary lubricating film does not exist, as expected of a simple n-alkane. Large fluctuations in friction coefficient suggest that surface wear is occurring. The sample is then heated at a rate of 1 °C min^{-1}. During heating there is a sudden transition to smooth sliding and lower friction at 122 °C. The ECR remains at 0 %. The friction coefficient remains steady and shows gradual decrease upon further sliding and continued heating to 150 °C. When the temperature eventually reaches 150°C, the ECR begins to show gradual increase, which continues throughout the test until an average ECR of 82 % is reached. Upon subsequent cooling back to 100 °C, the friction coefficient remains low and steady, thus the transition to lower friction and smooth sliding is irreversible. This indicates a permanent chemical change of n-hexadecane has occurred. Similar behaviour was observed in a repeat test, however, the transition to lower friction occurred at a higher temperature of 134 °C, SI Fig S1. It is hypothesized that high temperature results in thermal degradation of n-hexadecane, generating new polar species in the oil. These new polar species, being surface active, then adsorbed to steel surfaces forming low friction boundary films. Spectroscopic analysis of thermally degraded n-hexadecane is carried out in section 3.2 to test this hypothesis.

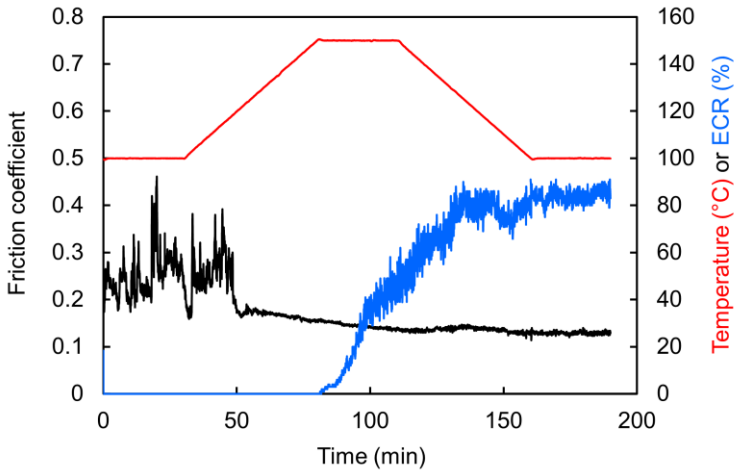


Fig 1. Impact of high temperature on the friction of n-hexadecane. Graph shows friction coefficient (black) and ECR (blue) for steel ball-steel disc sliding in hexadecane during heating-cooling cycle from 100 to 150°C (red).

3.2 Thermal degradation of n-hexadecane

Thermal degradation of n-hexadecane was carried out on a hotplate at temperatures of 130, 140, 145, 150, 170 and 190 °C. During degradation, aliquots were taken at intervals. The original hexadecane sample was colourless and odourless. Degraded hexadecane samples were also colourless but had a strong nutty odour, suggesting oxidation had occurred.

UV-vis spectroscopy reveals that clean n-hexadecane does not absorb in the tested range of 240-900 nm; this is expected since it does not contain groups that would give rise to electronic transitions at these energies. Degraded samples absorb in the UV part of the spectrum (240-300 nm), with λ_{max} = 271 nm, Fig 2 (a). Absorbance in this region is likely due to π-π* transitions of C=C bonds or n-π* transitions of C=O bonds. Double bond conjugation may push π-π* transitions, including those of C=O bonds, to lower energies (longer wavelengths) within the observed range of absorbance. The observed peak is a shoulder on another much larger peak (see also SI Fig S3); however, this has λ_{max} < 240 nm, outside the range of our measurements. Absorbance increases with aging time and degradation temperature, see SI Fig S2 for UV-vis spectra of samples aged at different temperatures. The spectrum appears noisy at longer aging times; this is an artefact of the spectrometer when measurements are made near the detection limit.

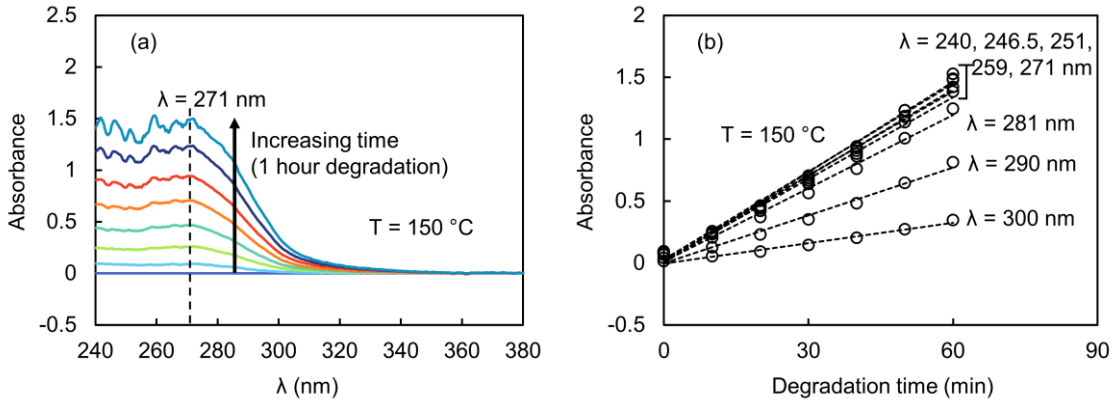


Fig 2. UV-vis spectroscopy of thermally degraded n-hexadecane. (a) UV-vis spectra showing changing properties of n-hexadecane during thermal degradation at 150°C and (b) change in absorbance with degradation time

UV-vis spectra have an approximately similar shape irrespective of aging temperature and time, see SI Fig S3. This suggests that roughly similar chemical groups are formed during aging at different temperatures, and that the main difference is in the rate of formation of these UV active species. Note that since UV-vis absorptions are by nature broad, and that the expected products of n-hexadecane degradation (e.g. ketones and aldehydes) will absorb in the same UV region, this technique may not be expected to differentiate between these different chemistries. (Clearer insight into the chemistries formed is afforded by FTIR and NMR spectroscopy, presented later.) For a given wavelength, a plot of absorbance vs. aging time can be made, Fig 2 (b). The relationship is found to be linear at all temperatures except at the lowest tested temperature of 130 °C. At 130 °C, negligible increase in absorbance is observed at short degradation times of 1 h, however, at longer degradation times (up to 4 hours), absorbance increases more sharply, suggesting that in this case, there is an

induction period where the rate increases exponentially with time, SI Fig S4. The gradient of the absorbance-aging time plot gives the effective rate of formation of species which absorb at this wavelength. From Beer-Lambert law:

$$A = \varepsilon c l$$

where A is absorbance, ε is the molar attenuation coefficient, c is the molar concentration and l is the path length. Given that a fixed path length of 1 cm was used and assuming that among tests, the species absorbing at a given wavelength have a similar molar attenuation coefficient, we can determine the effective concentration of degradation products, i.e. $A \propto c$. Since ε is not known, concentration and thus the calculated rates of formation of these degradation products are both in arbitrary units.

The Arrhenius equation can now be used to relate the reaction rate constant (k) to temperature (T):

$$k = Be^{-E_a/RT}$$

where B is the pre-exponential factor, E_a is the activation energy and R is the gas constant. An Arrhenius plot of $\ln(k)$ vs. $1/T$ is created for hexadecane degradation based on UV-vis data, Fig 3. It is found that there are two distinct regions. At lower temperatures, degradation rate increases with T. However, at higher temperatures, above 150°C, rate increases only slightly with T. Note, we plot absorbance data for λ = 300 nm, since this falls below the UV-vis saturation limit for all samples. However, similar-shaped plots were obtained irrespective of the selected wavelength, SI Fig S5. The gradient of the Arrhenius plot is equivalent to $(-E_a/R)$ and, since R is a constant, can be used to obtain the activation energy of the reaction. The activation energy for formation of degradation product appears higher (steeper slope) at lower temperatures than higher temperatures. Typically, activation energy is independent of temperature. Thus, a change in activation energy, as observed in our experiments, may suggest a change in the rate determining step.

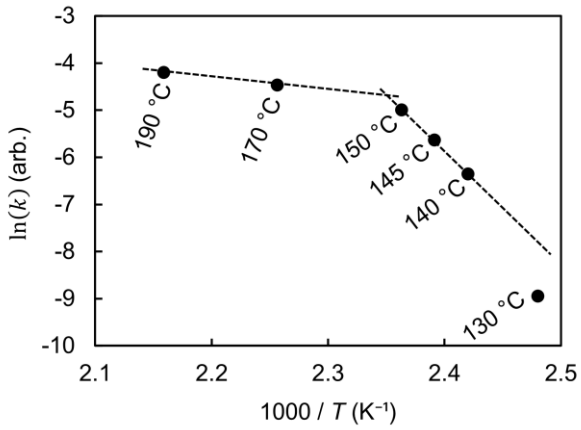


Fig 3. Arrhenius-type plot derived from UV-vis absorbance at 300 nm showing changing apparent rate of n-hexadecane degradation with temperature. Rate is calculated for 1 h degradation time.

Hydrocarbon autooxidation follows a free radical pathway and initiation involves the reaction of alkane (RH) with oxygen (O_2) to form hydroperoxide radical (HOO•) and alkyl radical (R•); this may be promoted by high temperature and / or light. It has been suggested the rate-limiting step in the early stages of hydrocarbon oxidation is the accumulation of hydroperoxides.[40] At higher temperatures, decomposition of hydroperoxides means that their concentration reaches a dynamic equilibrium, this may explain why at high temperatures above 150 °C the rate appears almost constant with temperature. Alternatively, oxidation products that form during heating to higher set temperatures may promote n-hexadecane autooxidation by alternative routes, lowering the activation energy. Other factors, like supply of oxygen, may also limit the rate of reaction.[6] Note that thermal degradation was not carried out under reflux, thus there may be more loss of degradation products by evaporation at higher temperatures, which could impact our results.

FTIR spectra were obtained of the degraded hexadecane samples prepared as thin squeeze films between KBr windows, Fig 4. Spectra were baseline corrected and normalised to the CH_2 asymmetric stretching peak at 2928 cm^{-1}. On first inspection the spectra appear identical to that of the clean hexadecane. However, a very small C=O stretching peak is observed at 1721 cm^{-1} for samples degraded at 150, 170 and 190 °C, suggesting the presence of carboxylic acid, aldehyde or ketone groups, Fig 5. Note that the low concentration of carbonyl species and the short pathlength, means that the signal to noise ratio is low. The carbonyl peak area is found to increase with aging time, Fig 5 (d), in agreement with the UV-vis results.

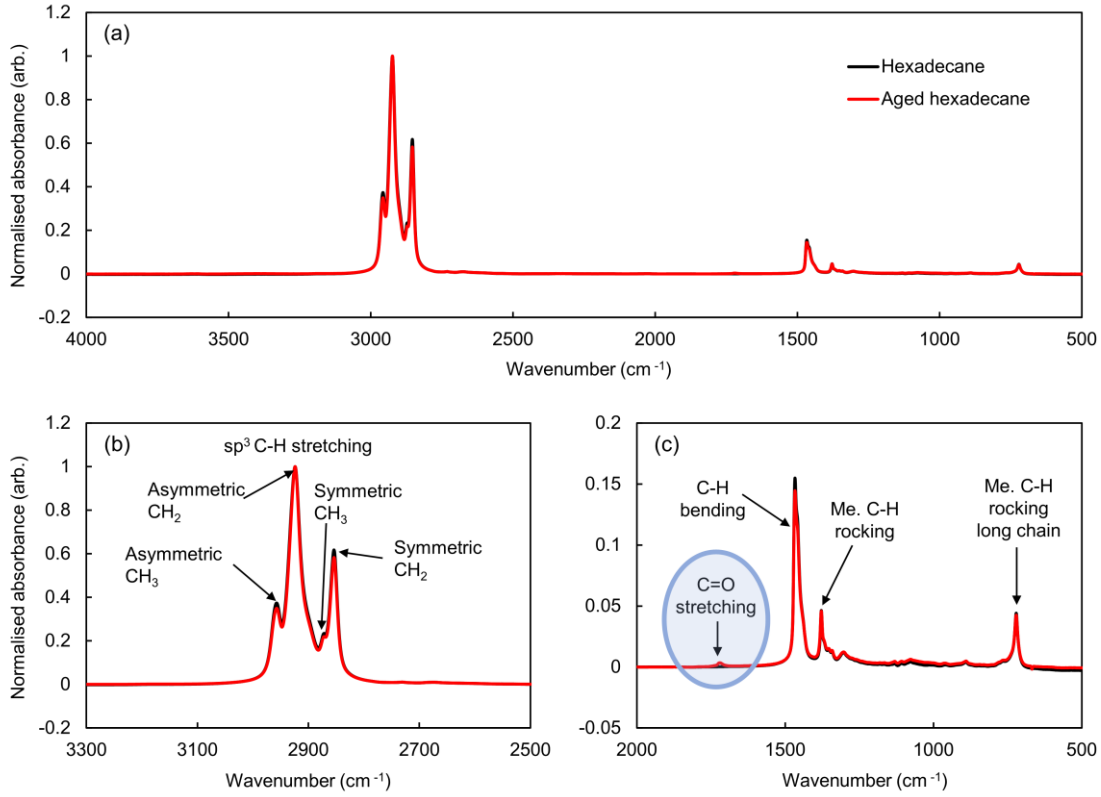


Fig 4. FTIR spectra of clean n-hexadecane and degraded n-hexadecane (1 h at 190 °C): (a) full spectra, (b) detail of CH stretching region and (c) low frequency region with band assignments.

Samples were prepared as thin squeeze films between KBr windows and acquired spectra are normalised to the asymmetric CH_2 stretching peak. Note that the carbonyl peak (circled) is only just visible.

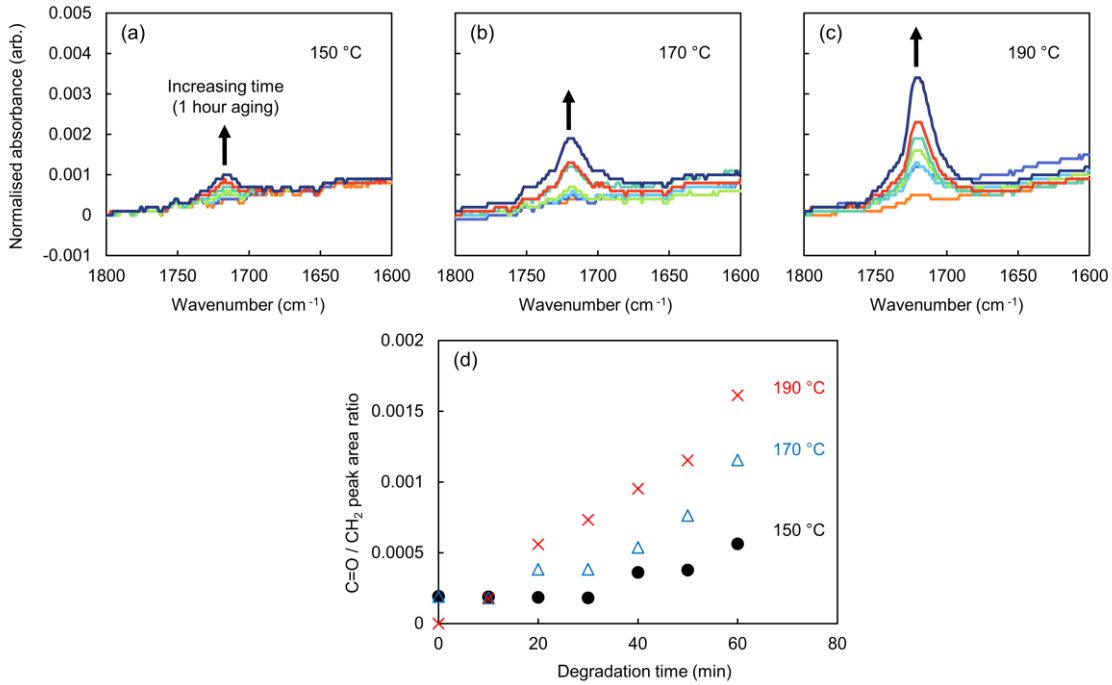


Fig 5. FTIR spectra showing the carbonyl stretching region for the aliquots taken during thermal degradation of n-hexadecane at (a) 150, (b) 170 and (c) 190 °C. (d) Carbonyl peak area vs. degradation time for experiments at different temperatures. Samples were prepared as thin squeeze films between KBr windows and acquired spectra are normalised to the asymmetric CH_2 stretching peak.

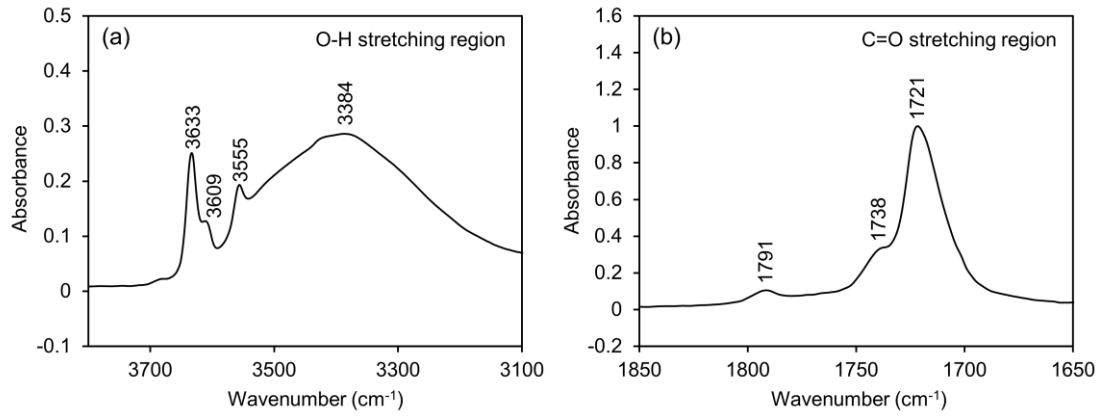


Fig 6. FTIR spectrum of n-hexadecane degradation products obtained by subtracting the spectrum of clean hexadecane from that of degraded hexadecane. (a) O-H and (b) C=O stretching regions. KBr windows, 1 mm pathlength. Sample was degraded for 1 h at 190°C.

FTIR spectra of clean n-hexadecane and a sample which had been degraded at 190°C for 1 h were obtained using a longer 1 mm pathlength, SI Fig S6. Note that certain peaks are saturated (e.g. C-H

stretching and bending), however, peaks arising from functional groups within the degradation products are stronger and more easily observed. The FTIR spectrum of the degradation products, shown in Fig 6, is obtained by subtracting the spectrum of clean n-hexadecane from that of degraded hexadecane. A broad peak at 3384 cm^{-1} is assigned to O-H stretching of H-bonded hydroxyl groups (alcohols and carboxylic acids), Fig 6 (a). Additional sharp peaks are assigned to O-H stretching of non-H-bonded hydroxyl groups; these occur at 3633 (1° or 2° alcohol), 3609 (phenol or aromatic alcohol) and 3555 (carboxylic acid) cm^{-1}. A peak at 1721 cm^{-1} is assigned to C=O stretching of a carbonyl group, perhaps within a ketone or carboxylic acid group. This peak is quite broad and has a shoulder at 1738 cm^{-1}, which may be assigned to aldehyde or ester. We infer that multiple carbonyl-containing groups are present within the degraded hexadecane. A smaller peak at 1791 cm^{-1} could perhaps be assigned to C=O stretching of a 'free' non-H-bonded acid, however the wavenumber is higher than that typically observed; this peak may also be due to more highly oxidised species such as acid anhydrides (which should display two different C=O stretching modes) or peroxy acids. Note that the asymmetric and symmetric C-H stretching peaks of the (O=)C-H aldehyde group, which usually occur at 2850 and 2750 cm^{-1} are not observed (SI Fig S6 bottom); these would be obscured by the shoulder of the strong n-alkane C-H stretching peaks. Numerous and overlapping peaks are observed within the fingerprint region; some of these may be assigned to O-H bending (1408 and 1327 cm^{-1}), C-O stretching (1243, 1128, 1063 and 1019 cm^{-1}), C=C bending (965 and 937 cm^{-1}) and sp^2 C-H bending (843 cm^{-1}), SI Fig S7. Repeat FTIR measurements are given in SI Fig S8.

^{1}H-NMR of clean n-hexadecane and the sample degraded for 1 h at 190 °C showed the expected 2 peaks corresponding to the 2 different hydrogen environments, δ 1.26 (s, 28H, CH_2) and 0.88 (t, 6H, CH_3, J = 6.8 Hz), see SI Fig S9. For the degraded hexadecane some very small additional peaks are observed in the baseline suggesting additional hydrogen environments, these are given in SI Table S1. A small peak at 9.8 ppm is assigned to aldehyde H. Peaks at ~7 ppm suggest that aromatic species are present. Peaks at ~4 ppm are assigned to H on carbon that is bonded to oxygen (e.g. on the carbon of an alcohol, ether, or alkoxy moiety of an ester). Peaks at c. 2.4 ppm are assigned to the α-H of carbonyl groups (e.g. on the carbon next to a carboxylic acid, ketone, aldehyde, or ester). Interestingly, the presence of aromatic species in the degradation products reported here was not observed in previous n-alkane thermal degradation studies.[41,42] However, these studies bubbled oxygen gas through the oil during degradation, while here we did not. Elsewhere, aromatic and light polycyclic aromatic hydrocarbons were observed after the autooxidation of sunflower oil at room temperature under oxygen-deficient conditions.[43]

Viscosity and density data are plotted in SI Fig S10. The viscosity of degraded hexadecane is slightly higher than that of clean hexadecane; dynamic viscosity at 100 °C is 0.898 and 0.915 mPa·s for clean n-hexadecane and thermally degraded n-hexadecane (1 h at 190 °C) respectively, see SI Table S2. For the same samples, density is also slightly increased from 0.7178 to 0.7210 g cm^{-3}, SI Table S3. Increased viscosity may be due to the formation of higher molecular weight "polymeric" degradation products or to 'simple' primary degradation products which, having polar groups, exhibit increased and stronger intermolecular bonding than the weak Van-der-Waals forces present in a simple n-

alkane.[44,45] Note that the increase in viscosity is relatively small; see that for our samples, viscometer temperature (90 vs. 100 °C) has a far greater impact on hexadecane viscosity than the presence of degradation products, SI Fig S10 (e).

3.3 Surface adsorption of n-hexadecane degradation products

QCM-D was used to monitor the adsorption of thermally degraded n-hexadecane (1 h at 190 °C) onto an Fe_2O_3 surface. At initial time, in clean n-hexadecane, stable baselines are observed for frequency and dissipation, Fig 7 (a). As degraded n-hexadecane is introduced there are negative shifts in frequency ($\Delta f_n/n$) and positive shifts in dissipation (ΔD_n). These are due to a combination of mass adsorption onto the Fe_2O_3 surface and liquid-loading effects. After 50 min, the surface is rinsed by flowing clean n-hexadecane (labelled 'R' in Fig 7). The data is corrected for liquid-loading and the adsorbed mass is approximated using the Sauerbrey equation.[46,47] The rate of adsorption is fast at initial time and slower at longer time, Fig 7 (b). The adsorbed mass does not plateau within 50 min and an equilibrium adsorbed amount is not reached. This likely suggests that multilayer adsorption is occurring, however, since the chemistry (and mass) of adsorbing species is not known, this cannot be confirmed. Rinsing with clean n-hexadecane results in mass loss, indicating that at least a proportion of the degradation products are physisorbed and readily removed. At longer rinse times, desorption continues at a much slower rate. After 40 min of rinsing, 43% of the total adsorbed mass remains on the surface, suggesting that this proportion of the film is strongly adsorbed and / or exhibits very slow dynamics of desorption.

In another test, the concentration of degradation products was sequentially increased, Fig 7 (c). Degraded n-hexadecane was diluted with clean n-hexadecane to obtain solutions of different concentration (vol %). It is observed that the degradation products adsorb onto the Fe_2O_3 surface even when they are present in the oil at lower concentrations, Fig 7 (d).

It is of interest to determine the adsorption kinetics of the degradation products, since these species will compete for surface sites with additives present in formulated lubricants. Preliminary tests made at liquid flow rates of up to 20 μLs^{-1} showed that initial rate of adsorption for thermally degraded n-hexadecane (undiluted) increased with increasing flow rate, Fig 8. Thus, for the tested range of flow rates, the initial rate of adsorption is mass transport-limited, and the adsorption kinetics cannot be obtained.

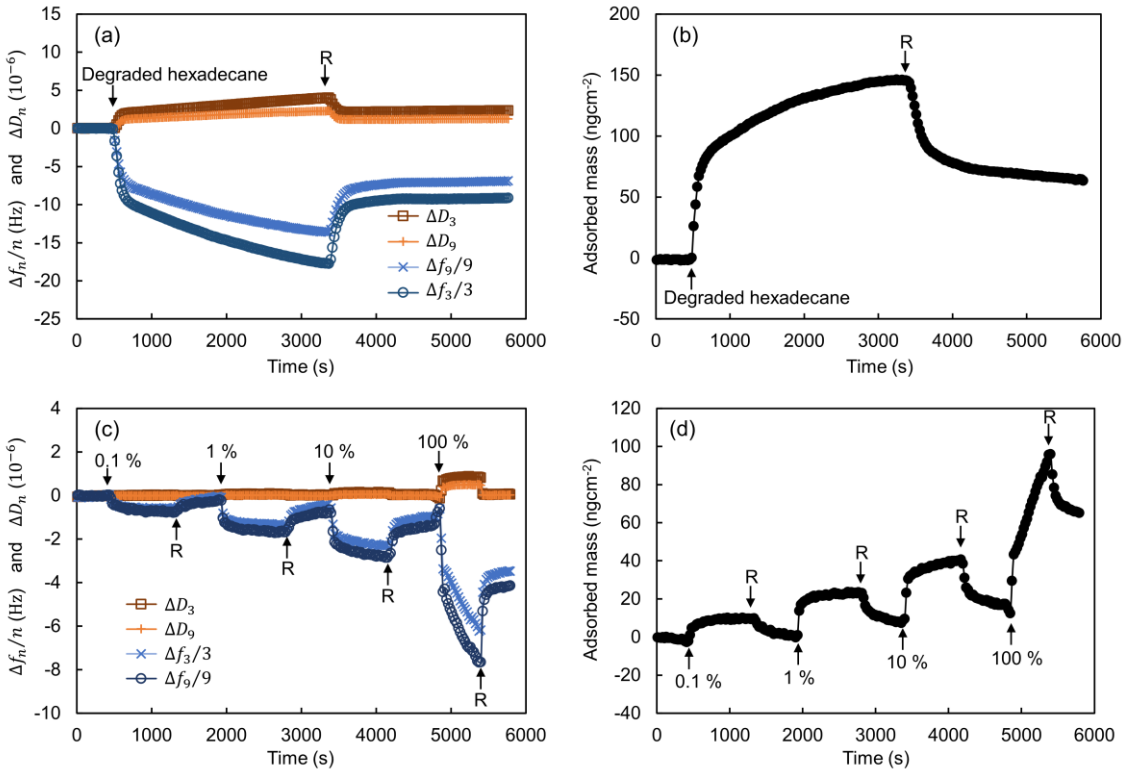


Fig 7. Adsorption of degraded n-hexadecane onto an Fe_2O_3 surface by QCM-D: (a,b) single adsorption-rinsing and (c,d) sequential increase in concentration of degraded hexadecane from 0.1 to 100 vol %. Baselines and rinsing steps (denoted 'R') are carried out in clean n-hexadecane. Flow rate = 2μLs^{-1} and temperature = 60°C.

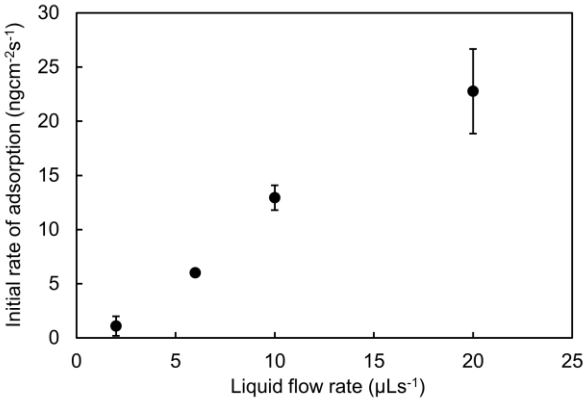


Fig 8. Initial rate of adsorption onto Fe_2O_3 from thermally degraded n-hexadecane at different liquid flow rates through the QCM-D at 60°C. Error bars show +/- 2 standard deviations of mean value from 3 tests.

3.4 Effect of base oil thermal degradation on its friction and wear-reducing properties

The friction and wear behaviour of clean n-hexadecane was compared to that of degraded n-hexadecane (1 h at 190 °C) by carrying out 3 h friction tests at constant temperature, Fig 9. At 100 °C

clean n-hexadecane exhibits high and unsteady friction (friction coefficient = 0.3 - 0.8). The ECR is ~ 0 %, suggesting that a boundary lubricating film does not form. At 150 °C, clean n-hexadecane exhibits low friction (friction coefficient = 0.11). The ECR increases with time from 0 to 97%, suggesting that boundary lubricating film thickness (or surface coverage) increases gradually with sliding. Degraded n-hexadecane at 100 °C exhibits similarly low friction (friction coefficient = 0.12). The ECR is high (~80 %) from the start of the test, suggesting that a boundary lubricating film forms instantaneously, likely owing to the ready availability of polar species like carboxylic acids in the degraded oil and their adsorption onto steel surfaces. The HFRR tests show good repeatability, SI Fig S11.

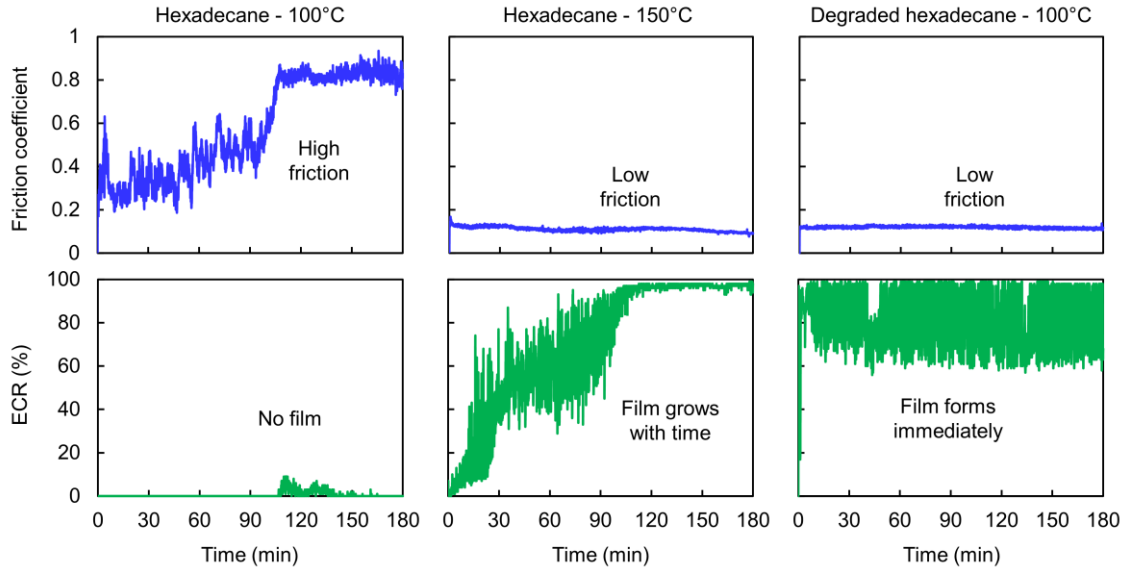


Fig 9. Impact of n-hexadecane thermal degradation on its friction. Graphs show friction coefficient (top) and ECR (bottom) during 3 h sliding of steel ball-steel disc in clean n-hexadecane at 100°C, clean n-hexadecane at 150°C and degraded n-hexadecane at 100°C.

Optical microscopy of the ball and disc reveal that wear scars form on both surfaces in all tests, Fig 10. The wear scars are significantly smaller for the tests made at 150°C with clean n-hexadecane and at 100°C with degraded n-hexadecane, i.e. the tests where low friction was observed. Friction and wear results are summarised in Table 1. Thick black deposits are observed outside the rubbed area, these are most prolific for the test made at 150°C. It is hypothesized that deposits are not simply metallic or metal oxide wear debris, but rather contain a considerable proportion of organic or organometallic material formed by hexadecane degradation inside the sliding contact. Note that the test with hexadecane at 100°C, which has the largest wear scar, generates the least amount of deposit, which supports that the deposits are at least partly organic, rather than simply metallic wear debris. Given the concentration of deposits around the wear scars, it is hypothesized that sliding promoted hexadecane degradation, above that obtained by thermal aging alone, as was suggested in a previous study.[21] Alternatively, or additionally, the sliding contact may have acted to concentrate insoluble deposits around the rubbed region. This may have been exacerbated by loss of liquid

lubricant volume for the test at 150°C – after the 3 h test the lubricant basin was almost completely dry.

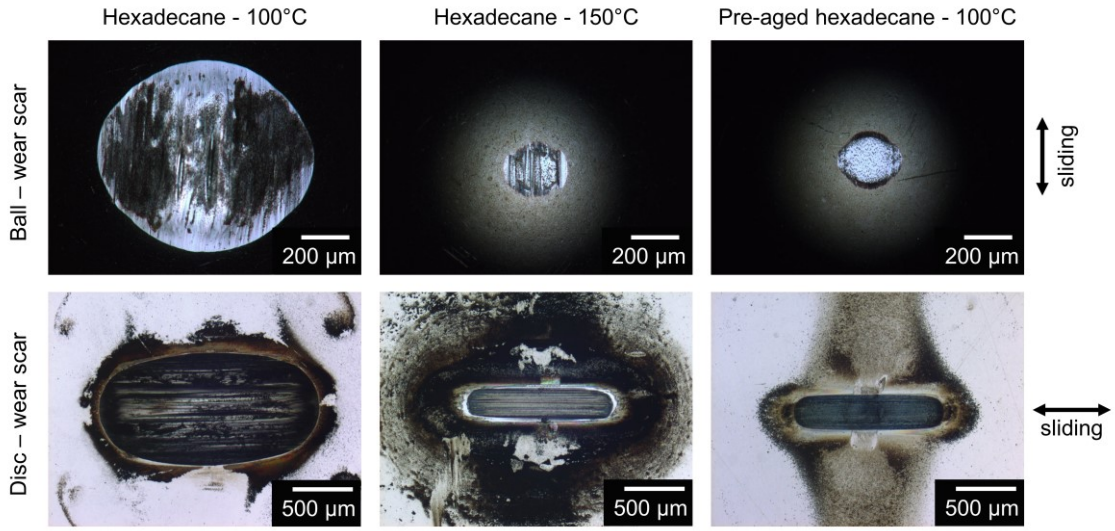


Fig 10. Impact of n-hexadecane thermal degradation on steel surface wear and deposit formation. Optical micrographs show surface of ball (top) and disc (bottom) after 3-hour sliding in n-hexadecane at 100°C, n-hexadecane at 150°C and degraded n-hexadecane at 100°C.

Table 1. Summary of friction and wear results for 3 h tests in hexadecane at 100°C, hexadecane at 150°C and degraded hexadecane at 100°C.

Lubricant	Friction test temperature (°C)	Mean friction coefficient	Std. Dev. friction coefficient	Mean ECR (%)	Mean wear scar diameter on ball (µm)
Hexadecane	100	0.581	0.448	0	925
Hexadecane	150	0.111	0.020	70	265
Degraded hexadecane	100	0.120	0.010	81	273

ATR-FTIR was carried out on the disc surface after the test at 150°C with hexadecane, see Fig 11. Spectra were acquired at different locations including (1) inside the wear scar, (2) in the thick deposit just outside the wear scar and (3) a region on the disc away from the wear scar which appeared to have no deposits (denoted as the clean area). Peaks corresponding to O-H stretching (α), C-H stretching (β and γ) and C=O carbonyl or CO_2^- carboxylate stretching (δ, ε, ζ, η, ι and κ) are observed (see peak annotations in Fig 11). To aid comparison, spectra are normalised to the maximum peak height, which is variable, not to the sp^3 C-H stretching, since the latter overlaps with the broad O-H stretching peak. The relative proportions of O-H and CO_2^- stretching to CH_2 stretching appears to

increase in the order: edge of disc (clean area) < thick deposits < inside wear scar. Thus, a greater proportion of polar species exist in and around the rubbed area.

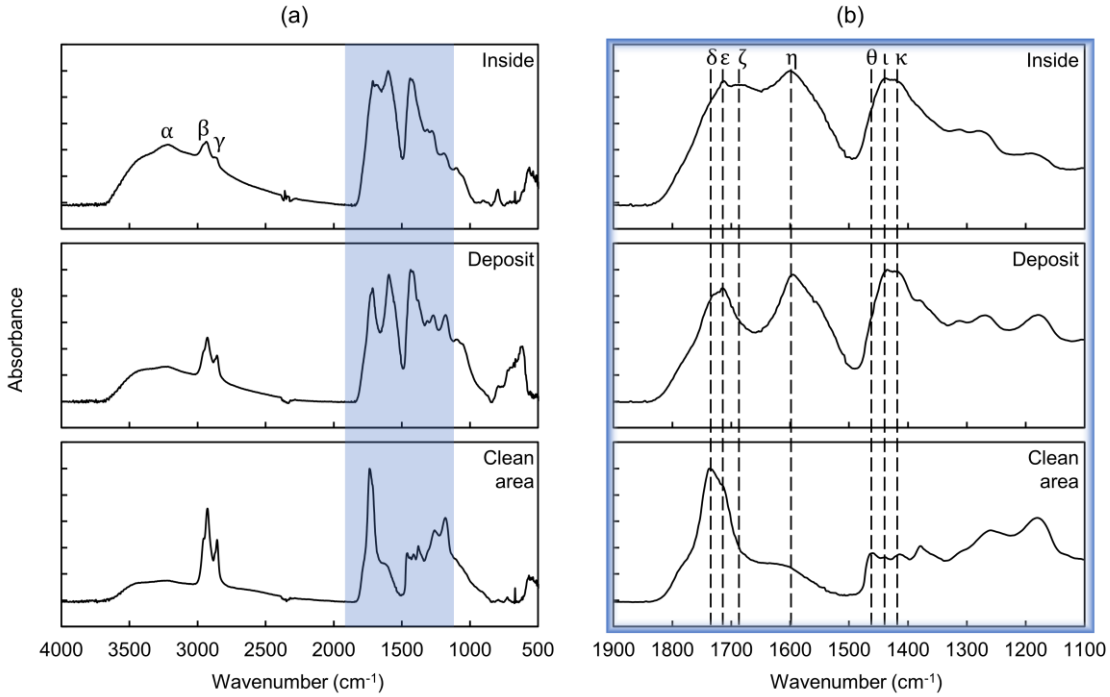


Fig 11. ATR-FTIR spectra of steel disc after 3 h sliding friction test at 150°C in hexadecane. Spectra are acquired inside the wear scar (Inside), in the thick black deposit (Deposit) and a clean area on the disc that appears to have no deposit (Clean area). Region highlighted in blue is expanded (right). Peaks annotated by Greek letters are assigned in Table 2.

Interestingly, different chemistries are observed at different locations on the disc surface, see Table 2 for IR band assignments. In the clean area, bands are observed at 1736 (δ) and 1713 (ε) cm^{-1}, assigned to C=O stretching of aldehyde or ester and H-bonded acid or ketone respectively. Inside the thick deposited film and the wear scar, additional bands, assigned to CO_2^- carboxylate asymmetric (η, 1598 cm^{-1}) and symmetric (ι, 1439 and κ, 1415 cm^{-1}) stretching, are observed. The splitting of the asymmetric and symmetric bands can be used to determine the mode of carboxylate binding to metal centres.[48,49] A splitting of 159-183 cm^{-1} suggests bridging binding, where each oxygen of the carboxylate binds to a different metal centre. This agrees with the reported mode of binding for iron (III) acetate,[50] and suggests the formation of polynuclear clusters or complexes containing multiple iron centres.[51] Thus, it can be inferred that the sliding contact acted to promote chemical reactions including the formation of iron carboxylates. Note that these carboxylates need not necessarily be bound directly to iron centres on the surface of the steel disc but may exist as a deposited film of coordination complexes with colloidal iron particles or iron ions created by wear of the steel surfaces.

Inside the wear scar an additional band is observed at 1679 - 1659 cm^{-1} (ζ) which is not observed elsewhere; this could possibly be assigned to C=C stretching of an alkene or even graphite-like amorphous carbon. Interestingly, these unsaturated species are only found inside the wear scar,

which was potentially more oxygen-starved (anaerobic) than elsewhere on the disc owing to contact with the ball counter-surface. Alternative assignments of this same peak could be CO_2^- asymmetric stretching of a metal-coordinated aromatic acid [52] or C=O stretching of an aromatic aldehyde or aromatic ketone.[53,54] Although amides also have a band in this region, a clear mechanism for the formation of amides during the thermal / mechanochemical degradation of n-hexadecane cannot be found. Repeat ATR-FTIR spectra are given in SI Fig S12.

The deposited film formed after a 1 h HFRR test made at 100°C using pre-aged n-hexadecane (aged on hotplate for 1 h at 150°C), displayed a similar micro-reflectance FTIR spectrum to a deposited film formed after a 1 h HFRR test made at 150°C, SI Fig S13. This proves that simultaneous high temperature (150°C) and rubbing is not necessary to form iron carboxylates. Polar species (acids, esters, alcohols) can be formed by thermal degradation without a steel surface or frictional contact. Subsequent tribochemical reaction to form iron carboxylates will then proceed at 100°C, and likely even lower temperatures, as has been seen with fatty acid-type friction modifiers.[55]

Iron carboxylates have previously been observed on steel friction surfaces after sliding in n-hexadecane [56–58]. The temperature of the friction test was found to impact the chemistries found on the surface.[57] FTIR peaks were observed at 1740 and 1600 cm^{-1} for a test made at 200 °C and 1650 and 1550 cm^{-1} for a test made at 20 °C.

Note that in the FTIR spectra of the disc surface, the C=O stretching peaks are very large respective to other bands (e.g. C-H stretching), this is contrary to the FTIR transmission spectra of the degraded liquid hexadecane samples, where the carbonyl peak was small by comparison to C-H stretching (Fig 4). This hints at preferential adsorption of polar degradation products to the steel surface, a catalytic effect of the steel surface, and tribo-chemical contribution during n-hexadecane degradation.

To determine whether the frictional steel-steel contact promotes n-hexadecane degradation, two shorter 1 h tests were carried out in the HFRR at 150°C – one with sliding and one without (in which the ball-disc contact was static). A visible wear scar and deposited film is observed on the disc which was rubbed, while the unrubbed disc appears clean with no visible deposit. Transmission FTIR of the liquid lubricants using a 1 mm pathlength reveals that the degradation products existing in the n-hexadecane are similar for the two tests, SI Fig S14. Unexpectedly, the absorbance of C=O and O-H stretching is marginally higher for the test without rubbing. Micro-reflectance FTIR (100 µm aperture) of the steel disc surfaces reveals that iron carboxylates form only on the disc which was rubbed. The spectra of the unrubbed disc are featureless, suggesting no organic or organometallic film exists, SI Fig S15. Note that this technique is insensitive to very thin films, such as monolayers. In short, there is scant evidence that the rubbing contact promoted bulk n-hexadecane oxidation above that seen under similar conditions without rubbing. However, interpretation is not straightforward since although the concentration of polar degradation products existing in the liquid phase is slightly higher for the test without rubbing, the total amount of polar species formed may in fact be the same or higher for the test with rubbing. This is because polar degradation products existing in the liquid phase may be entrained into the sliding contact and undergo tribochemical reaction to form insoluble iron

carboxylates, these then precipitate onto the steel surface (as seen by micro-reflectance FTIR), thereby depleting the concentration of degradation products dissolved in the bulk liquid phase.

In summary, this study has shown that pre-aging of n-hexadecane on a hotplate created polar degradation products that formed a boundary lubricating film which gave reduced friction and wear relative to clean n-hexadecane in tests at 100°C. Alternatively, a boundary film could be formed by combined tribo- and thermally-promoted degradation of n-hexadecane in situ during the friction test at a higher test temperature of 150 °C.

Table 2. ATR-FTIR absorptions for steel disc after 3 h sliding friction test at 150°C in hexadecane. Spectra are acquired inside the wear scar (Inside), in the thick black deposit (Deposit) and a clean area on the disc that appears to have no deposit (Clean area). 'br', 's' and 'w' denote broad, strong and weak absorptions respectively. Relative peak heights, normalised to the maximum absorption in the spectrum without peak deconvolution, are given as a rough guide – they cannot be used to obtain the exact proportions of the chemistries present. Bands are assigned to stretching (ν) and bending (σ) modes. *Band may be hidden by overlapping adjacent bands.

IR absorption band (cm^{-1})	Relative peak height			Assignment	Peak annotation in Fig. 11
	Inside	Deposit	Clean Area		
3214 br	0.44	0.26	0.15	ν (OH)	α
2956	0.44	0.38	0.47	ν_{as} (CH_3)	
2928	0.45	0.49	0.70	ν_{as} (CH_2)	β
2872	0.34	0.32	0.36	ν_s (CH_3)	
2857	0.33	0.35	0.46	ν_s (CH_2)	γ
1736 s	0.76	0.76	1.00	ν (C=O) *Aldehyde*	δ
1713 s	0.92	0.86	0.86	ν (C=O) *H-bonded acid or Ketone*	ε
1679 - 1659 s	0.87			ν (C=C) Alkene	ζ
1598 s	1.00	0.96		ν_{as} (CO_2^-)	η
1462 w	*	*	0.36	σ (CH_2)	θ
1439	0.94	1.00	0.33	ν_s (CO_2^-)	ι
1415	0.92	0.98	0.35	ν_s (CO_2^-)	κ
1378	*	0.76	0.41	σ (CH) *Aldehyde*	
1313 w	0.55	0.61	0.36	σ (OH) *Phenol*	
1266 w	0.52	0.65	0.53	ν (C-O) *Aromatic ester*	
1179		0.66	0.63	ν (C-O) *Ester or Alcohol*	

4 Conclusions

Upon heating n-hexadecane from 100 to 150 °C during an HFRR sliding friction test between a steel ball and disc, a transition from high to low boundary friction occurs at 122-134 °C. A gradual increase in boundary film thickness or surface-coverage is indicated by rising electrical contact resistance between the ball and disc. Thermally degraded n-hexadecane samples were prepared by heating n-hexadecane in air on a hotplate at temperatures of 130-190 °C. These samples absorb in the near to mid UV region, suggesting the presence of C=C and/or C=O groups. UV absorbance increases with degradation time and temperature and may thus be used to approximate rate of oil oxidation. FTIR and ^{1}H NMR spectroscopy reveal the presence of polar oxidation products (aldehydes, carboxylic acids, ketones, esters and alcohols) as well as some unsaturated (alkene and aromatic) molecules.

n-Hexadecane that has been thermally degraded in air on a hotplate gives lower boundary friction and lower wear than clean n-hexadecane during HFRR tests at 100 °C. Degraded n-hexadecane has almost negligible viscosity increase relative to clean n-hexadecane. Thus, improved lubricity is explained by chemical rather than physical changes to the oil. QCM-D adsorption studies confirm that n-hexadecane degradation products adsorb onto Fe_2O_3 surfaces, forming a film where a proportion of the adsorbed material is strongly adsorbed, viz. not readily removed by rinsing with clean n-hexadecane. Low friction and wear are achieved by clean n-hexadecane during an HFRR test at a higher temperature of 150 °C. In this case oil oxidation occurs in situ during the friction test. Iron carboxylates (bridging bidentate) are observed exclusively inside the wear track and the thick deposit around its periphery, suggesting that the rubbing contact promotes iron complexation and that some reactions are tribochemical rather than purely thermal. Although thermal degradation of n-hexadecane base oil leads to improved lubricity when tested neat (without additives), the impact of degradation may be different in formulated oils. Since oxidation products are surface active and capable of forming boundary lubricating films, they may interfere with organic friction modifier additive adsorption from formulated lubricants.

Acknowledgements

The authors thank Prof. Philippa Cann for use of the FTIR spectrometer. C. W. J. F. was supported by Overseas Internship Scheme 2018, College of Engineering, City University of Hong Kong.

References

[1] Dörr N, Agocs A, Besser C, Ristić A, Frauscher M. Engine Oils in the Field: A Comprehensive Chemical Assessment of Engine Oil Degradation in a Passenger Car. Tribol Lett 2019;67:68.

https://doi.org/10.1007/s11249-019-1182-7.

[2] Gerry K. Base oil degradation and hydocarbon autoxidation, PhD Thesis. Imperial College London, 2009.

[3] Fuchs GH Von, Diamond H. Oxidation Characteristics of Lubricating Oils. Ind Eng Chem 1942;34:927–37. https://doi.org/10.1021/ie50392a007.

[4] Santos JCO, Santos IMG, Souza AG. Thermal Degradation Process of Synthetic Lubricating Oils: Part I-Spectroscopic Study. Pet Sci Technol 2015;33:1238–45. https://doi.org/10.1080/10916466.2015.1047031.

[5] Jin Y, Duan H, Wei L, Chen S, Qian X, Jia D, et al. Online infrared spectra detection of lubricating oil during friction process at high temperature. Ind Lubr Tribol 2018;70:1294–302. https://doi.org/10.1108/ILT-09-2017-0251.

[6] Jensen RK, Korcek S, Mahoney LR, Zinbo M. Liquid-Phase Autoxidation of Organic Compounds at Elevated Temperatures. 1. The Stirred Flow Reactor Technique and Analysis of Primary Products from n-Hexadecane Autoxidation at 120-180 °C. J Am Chem Soc 1979;101:7574–84. https://doi.org/10.1021/ja00519a018.

[7] Denisov ET, Khudyakov I V. Mechanisms of Action and Reactivities of the Free Radicals of Inhibitors. Chem Rev 1987;87:1313–57. https://doi.org/10.1021/cr00082a003.

[8] Hsu S, Ku C, Pei P. Oxidative Degradation Mechanisms of Lubricants. West Conshohocken, PA: ASTM International; 2008. https://doi.org/10.1520/stp18372s.

[9] Soleimani M, Dehabadi L, Wilson LD, Tabil LG. Antioxidants Classification and Applications in Lubricants. Lubr. - Tribol. Lubr. Addit., 2018. https://doi.org/10.5772/intechopen.72621.

[10] Blaine S, Savage PE. Reaction Pathways in Lubricant Degradation. 2. n-Hexadecane Autoxidation. Ind Eng Chem Res 1991;30:2185–91. https://doi.org/10.1021/ie00057a020.

[11] Aguilar G, Mazzamaro G, Rasberger M. Oxidative degradation and stabilisation of mineral oil-based lubricants. Chem. Technol. Lubr. Third Ed., 2010, p. 107–52. https://doi.org/10.1023/b105569_4.

[12] Wang Z, Popolan-Vaida DM, Chen B, Moshammer K, Mohamed SY, Wang H, et al. Unraveling the structure and chemical mechanisms of highly oxygenated intermediates in oxidation of organic compounds. Proc Natl Acad Sci U S A 2017;114:13102–7. https://doi.org/10.1073/pnas.1707564114.

[13] Hsu SM, Gates RS. Boundary lubricating films: Formation and lubrication mechanism. Tribol. Int., vol. 38, 2005, p. 305–12. https://doi.org/10.1016/j.triboint.2004.08.021.

[14] Naidu SK, Klaus EE, Duda JL. Evaluation of Liquid Phase Oxidation Products of Ester and Mineral Oil Lubricants. Ind Eng Chem Prod Res Dev 1984;23:613–9. https://doi.org/10.1021/i300016a021.

[15] Fenske MR, Stevenson CE, Lawson ND, Herbolsheimer G, Koch EF. Oxidation of Lubricating Oils. Factors Controlling Oxidation Stability. Ind Eng Chem 1941;33:516–24. https://doi.org/10.1021/ie50376a017.

[16] Hass HB, McBee ET, Churchill JW. Oxidation of Hexadecane. Ind Eng Chem 1945;37:445–8. https://doi.org/10.1021/ie50425a018.

[17] Hsu SM. Boundary lubrication: Current understanding. Tribol Lett 1997;3:1–11. https://doi.org/10.1023/A:1019152331970.

[18] Pignatello JJ, Oliveros E, MacKay A. Advanced oxidation processes for organic contaminant destruction based on the fenton reaction and related chemistry. Crit Rev Environ Sci Technol 2006;36:1–84. https://doi.org/10.1080/10643380500326564.

[19] He J, Yang X, Men B, Wang D. Interfacial mechanisms of heterogeneous Fenton reactions catalyzed by iron-based materials: A review. J Environ Sci (China) 2016;39:97–109. https://doi.org/10.1016/j.jes.2015.12.003.

[20] Antonio EN, Wicking C, Filip S, Ryan MP, Heutz S. Role of Iron Speciation in Oxidation and Deposition at the Hexadecane-Iron Interface. ACS Appl Mater Interfaces 2020;12:19140–52. https://doi.org/10.1021/acsami.9b22983.

[21] Singh A, Gandra RT, Schneider EW, Biswas SK. Lubricant degradation and related wear of a steel pin in lubricated sliding against a steel disc. ACS Appl Mater Interfaces 2011;3:2512–21. https://doi.org/10.1021/am200375a.

[22] Maduako AUC, Ofunne GC, Ojinnaka CM. The role of metals in the oxidative degradation of automotive crankcase oils. Tribol Int 1996;29:153–60. https://doi.org/10.1016/0301-679X(95)00013-T.

[23] Furlong O, Miller B, Kotvis P, Adams H, Tysoe WT. Shear and thermal effects in boundary film formation during sliding. RSC Adv 2014;4:24059. https://doi.org/10.1039/c4ra03519d.

[24] Tysoe W. On Stress-Induced Tribochemical Reaction Rates. Tribol Lett 2017;65:48. https://doi.org/10.1007/s11249-017-0832-x.

[25] Jahanmir S. Chain length effects in boundary lubrication. Wear 1985;102:331–49. https://doi.org/10.1016/0043-1648(85)90176-0.

[26] Jahanmir S, Beltzer M. An Adsorption Model for Friction in Boundary Lubrication. A S L E

Trans 1986;29:423–30. https://doi.org/10.1080/05698198608981704.

[27] Campen S. Fundamentals of Organic Friction Modifier Behaviour. PhD Thesis, Imperial College London, 2012.

[28] Bowden FP, Leben L, Tabor D. The influence of temperature on the stability of a mineral oil. Trans Faraday Soc 1939;35:900–4. https://doi.org/10.1039/tf9393500900.

[29] Besser C, Agocs A, Ronai B, Ristic A, Repka M, Jankes E, et al. Generation of engine oils with defined degree of degradation by means of a large scale artificial alteration method. Tribol Int 2019. https://doi.org/10.1016/j.triboint.2018.12.003.

[30] Fournet R, Battin-Leclerc F, Glaude PA, Judenherc B, Warth V, Come GM, et al. The gas-phase oxidation of n-hexadecane. Int J Chem Kinet 2001;33:574–86. https://doi.org/10.1002/kin.1053.

[31] Ristori A, Dagaut P, Cathonnet M. The oxidation of n-hexadecane: Experimental and detailed kinetic modeling. Combust Flame 2001;125:1128–37. https://doi.org/10.1016/S0010-2180(01)00232-2.

[32] Ratoi M, Anghel V, Bovington C, Spikes HA. Mechanisms of oiliness additives. Tribol Int 2000;33:241–7. https://doi.org/10.1016/S0301-679X(00)00037-2.

[33] Hamrock BJ, Dowson D. Isothermal Elastohydrodynamic Lubrication of Point Contacts: Part III-Fully Flooded Result. J Tribol 1977;99:264–75. https://doi.org/10.1115/1.3453074.

[34] Hartl M, Molimard J, Křupka I, Vergne P, Querry M, Poliščuk R, et al. Thin film lubrication study by colorimetric interferometry. Tribol Ser 2000;38:695–704. https://doi.org/10.1016/s0167-8922(00)80172-8.

[35] Glovnea RP, Forrest AK, Olver A V., Spikes HA. Measurement of sub-nanometer lubricant films using ultra-thin film interferometry. Tribol Lett 2003;15:217–30. https://doi.org/10.1023/A:1024809102533.

[36] Suresh AK, Sharma MM, Sridhar T. Engineering aspects of industrial liquid-phase air oxidation of hydrocarbons. Ind Eng Chem Res 2000;39:3958–97. https://doi.org/10.1021/ie0002733.

[37] Ribeiro FCP, Oliveira AS, Araújo A, Marinho W, Schneider MP, Pinto L, et al. Detection oxidative degradation in lubricating oil under storage conditions using digital images and chemometrics. Microchem J 2019;147:622–7. https://doi.org/10.1016/j.microc.2019.03.087.

[38] Kanazawa KK, Gordon JG. Frequency of a Quartz Microbalance in Contact with Liquid. Anal Chem 1985;57:1770–1. https://doi.org/10.1021/ac00285a062.

[39] Campen SM, Moorhouse SJ, Wong JSS. Effect of Aging on the Removal of Asphaltene Deposits with Aromatic Solvent. Langmuir 2019;35:11995–2008. https://doi.org/10.1021/acs.langmuir.9b01792.

[40] Blaine S, Savage PE. Reaction Pathways in Lubricant Degradation. 3. Reaction Model for n-Hexadecane Autoxidation. Ind Eng Chem Res 1992;31:69–75. https://doi.org/10.1021/ie00001a010.

[41] Boss BD, Hazlett RN. Oxidation of hydrocarbons in the liquid phase: n -dodecane in a borosilicate glass chamber at 200 °C . Can J Chem 1969;47:4175–82. https://doi.org/10.1139/v69-691.

[42] Blaine S, Savage PE. Reaction Pathways in Lubricant Degradation. 1. Analytical Characterization of n-Hexadecane Autoxidation Products. Ind Eng Chem Res 1991;30:792–8. https://doi.org/10.1021/ie00052a026.

[43] Guillén MD, Goicoechea E, Palencia G, Cosmes N. Evidence of the formation of light polycyclic aromatic hydrocarbons during the oxidation of edible oils in closed containers at room temperature. J Agric Food Chem 2008;56:2028–33. https://doi.org/10.1021/jf072974h.

[44] Chen CI, Hsu SM. A chemical kinetics model to predict lubricant performance in a diesel engine. Part I: Simulation methodology. Tribol Lett 2003;14:83–90. https://doi.org/10.1023/A:1021748002697.

[45] Diaby M, Sablier M, Le Negrate A, El Fassi M, Bocquet J. Understanding carbonaceous deposit formation resulting from engine oil degradation. Carbon N Y 2009;47:355–66. https://doi.org/10.1016/j.carbon.2008.10.014.

[46] Sauerbrey G. Verwendung von Schwingquarzen zur Wägung dünner Schichten und zur Mikrowägung. Zeitschrift Für Phys 1959;155:206–22. https://doi.org/10.1007/BF01337937.

[47] Tavakkoli M, Panuganti SR, Taghikhani V, Pishvaie MR, Chapman WG. Asphaltene Deposition in Different Depositing Environments: Part 2. Real Oil. Energy & Fuels 2014;28:3594–603. https://doi.org/10.1021/ef401868d.

[48] Bronstein LM, Huang X, Retrum J, Schmucker A, Pink M, Stein BD, et al. Influence of iron oleate complex structure on iron oxide nanoparticle formation. Chem Mater 2007;19:3624–32. https://doi.org/10.1021/cm062948j.

[49] Nakamoto K. Infrared and Raman Spectra of Inorganic and Coordination Compounds, Part B: Applications in Coordination, Organometallic and Bioinorganic Chemistry. 5th ed. New York: Wiley; 1997.

[50] NIST Chemistry WebBook, Standard Reference Data, IR Spectrum of Iron Acetate n.d.

https://webbook.nist.gov/cgi/inchi?ID=B6005557&Mask=80#IR-Spec.

[51] Abrahamson HB, Lukaski HC. Synthesis and characterization of iron stearate compounds. J Inorg Biochem 1994;54:115–30. https://doi.org/10.1016/0162-0134(94)80025-1.

[52] Zhang S, Jiao Z, Yao W. A simple solvothermal process for fabrication of a metal-organic framework with an iron oxide enclosure for the determination of organophosphorus pesticides in biological samples. J Chromatogr A 2014;1371:74–81. https://doi.org/10.1016/j.chroma.2014.10.088.

[53] Tolstorozhev GB, Skornyakov I V., Bel'kov M V., Shadyro OI, Brinkevich SD, Samovich SN. IR Spectra of benzaldehyde and its derivatives in different aggregate states. Opt Spectrosc (English Transl Opt i Spektrosk 2012;113:179–83. https://doi.org/10.1134/S0030400X12070247.

[54] Zhang S, Zhang C, Li K, Luo J. Investigation of ultra-low friction on steel surfaces with diketone lubricants. RSC Adv 2018;8:9402–8. https://doi.org/10.1039/c7ra13027a.

[55] Murase A, Ohmori T. ToF-SIMS analysis of model compounds of friction modifier adsorbed onto friction surfaces of ferrous materials. Surf Interface Anal 2001;31:191–9. https://doi.org/10.1002/sia.969.

[56] Makowska M, Kajdas C, Grądkowski M. Interactions of n-hexadecane with 52100 steel surface under friction conditions. Tribol. Lett., vol. 13, 2002, p. 65–70. https://doi.org/10.1023/A:1020192229898.

[57] Kajdas C, Makowska M, Gradkowski M. Influence of temperature on the tribochemical reactions of hexadecane. Lubr Sci 2003;15:329–40. https://doi.org/10.1002/ls.3010150405.

[58] Kajdas C, Makowska M, Gradkowski M. Tribochemistry of n-hexadecane in different material systems. Lubr Sci 2006;18:255–63. https://doi.org/10.1002/ls.22.